Implementation of a damage model in a finite element program for computation of structures under dynamic loading

Nasserdine Oudni
Department of civil engineering, faculty of technology, A. Mira University, Bejaia, Algeria
Laboratory of modeling of materials and structures, University of Tizi-Ouzou, Algeria
nasroudni@yahoo.fr

Youcef Bouafia
Laboratory of modeling of materials and structures, University of Tizi-Ouzou, Algeria
youcef.bouafia2012@yahoo.com

ABSTRACT. This work is a numerical simulation of nonlinear problems of the damage process and fracture of quasi-brittle materials especially concrete. In this study, we model the macroscopic behavior of concrete material, taking into account the phenomenon of damage. J. Mazars model whose principle is based on damage mechanics has been implemented in a finite element program written Fortran 90, it takes into account the dissymmetry of concrete behavior in tension and in compression, this model takes into account the cracking tensile and rupture in compression. It is a model that is commonly used for static and pseudo-static systems, but in this work, it was used in the dynamic case.

KEYWORDS. Damage; Dynamic; Modeling; Displacement; Strain; Local approach; Time integration; explicit; quasi-brittle.

INTRODUCTION

The numerical program is employed in analyzing Koyna gravity dam and comparing the results with available results of many researchers find in literature. The choice of Koyna concrete gravity dam is due to the fact that many studies have been done on this structure which experienced a devastating earthquake in 1967. Since Koyna dam in the 1967 Koyna earthquake [1-4] is one of the few examples of cracking in a concrete dam, it has been selected to investigate its earthquake response. The earthquake records are in the form of accelerograms with horizontal and vertical components which are used as dynamic loads. The effect of the damping coefficient is obviously taken into account.
This work proposes the implementation of a damage model based on the damage mechanics as part of the isotropic formulation proposed by J. Lemaitre in a finite element program. the J. Mazars model [5] whose principle is based on damage mechanics which is a theory describing the progressive reduction of the mechanical properties of a material due to initiation, growth and coalescence of microscopic cracks. These internal changes lead to the degradation of mechanical properties of the material. The model takes into account the asymmetry of concrete behavior and it considers the cracking in tension and compression failure. The method is based on the notion of equivalence of the strains.

MODEL

The influence of microcracking due to external loads is introduced via a single scalar damage variable d ranging from 0 for the undamaged material to 1 for completely damaged material. The stress-strain relation reads [6]:

$$\varepsilon_{ij} = \frac{1+\upsilon_0}{E_0(1-d)}\sigma_{ij} - \frac{\upsilon_0}{E_0(1-d)}\left[\sigma_{kk}\delta_{ij}\right] \tag{1}$$

E_0 and υ_0 are the Young's modulus and the Poisson's ratio of the undamaged material; ε_{ij} and σ_{ij} are the strain and stress components, and δ_{ij} is the Kronecker symbol. The elastic (i.e., free) energy per unit mass of material is

$$\rho\psi = \frac{1}{2}(1-d)\varepsilon_{ij}C^0_{ijkl}\varepsilon_{kl} \tag{2}$$

Where C^0_{ijkl} is the stiffness of the undamaged material. This energy is assumed to be the state potential. The damage energy release rate is

$$Y = -\rho\frac{\partial\psi}{\partial d} = \frac{1}{2}\varepsilon_{ij}C^0_{ijkl}\varepsilon_{kl} \tag{3}$$

With the energy of dissipated energy:

$$\dot{\phi} = -\frac{\partial\rho\psi}{\partial d}\dot{d} \tag{4}$$

Since the dissipation of energy ought to be positive or zero, the damage rate is constrained to the same inequality because the damage energy release rate is always positive.

DAMAGE EVOLUTION

The evolution of damage is based on the amount of extension that the material is experiencing during the mechanical loading. An equivalent strain is defined as

$$\tilde{\varepsilon} = \sqrt{\sum_{i=1}^{3}\left(\varepsilon_{i+}\right)^2} \tag{5}$$

Where $\langle . \rangle_+$ is the Macauley bracket and ε_i are the principal strains. The loading function of damage is

$$f(\tilde{\varepsilon},\kappa) = \tilde{\varepsilon} - \kappa \tag{6}$$

Where κ is the threshold of damage growth. Initially, its value is κ_0 , which can be related to the peak stress f_t of the material in uniaxial tension:

$$\kappa_0 = \frac{f_t}{E_0} \tag{7}$$

In the course of loading κ assumes the maximum value of the equivalent strain ever reached during the loading history.

$$If \quad f(\tilde{\varepsilon},\kappa)=0 \ \ and \ \ \dot{f}(\tilde{\varepsilon},\kappa)=0, \ Then \ \begin{cases} d=h(\kappa) \\ \kappa=\tilde{\varepsilon} \end{cases} \quad With\, \dot{d}\geq 0, \quad else \begin{cases} \dot{d}=0 \\ \dot{\kappa}=0 \end{cases} \tag{8}$$

The function $h(\kappa)$ is detailed as follows: in order to capture the differences of mechanical responses of the material in tension and in compression, the damage variable is split into two parts:

$$d=\alpha_t d_t+\alpha_c d_c \tag{9}$$

Where d_t and d_c are the damage variables in tension and compression, respectively. They are combined with the weighting coefficients α_t and α_c, defined as functions of the principal values of the strains ε_{ij}^t and ε_{ij}^c due to positive and negative stresses:

$$\varepsilon_{ij}^t=(1-d)C_{ijkl}^{-1}\sigma_{kl}^t, \quad \varepsilon_{ij}^c=(1-d)C_{ijkl}^{-1}\sigma_{kl}^c \tag{10}$$

$$\alpha_t=\sum_{i=1}^{3}\left(\frac{\varepsilon_i^t\varepsilon_i}{\tilde{\varepsilon}^2}\right)^{\beta}, \quad \alpha_c=\sum_{i=1}^{3}\left(\frac{\varepsilon_i^c\varepsilon_i}{\tilde{\varepsilon}^2}\right)^{\beta} \tag{11}$$

Note that in these expressions, strains labeled with a single indicia are principal strains. In uniaxial tension $\alpha_t=1$ and $\alpha_c=0$. In uniaxial compression $\alpha_c=1$ and $\alpha_t=0$. Hence, d_t and d_t can be obtained separately from uniaxial tests.
The evolution of damage is provided in an integrated form, as a function of the variable κ:

$$d_t=1-\frac{\kappa_0(1-A_t)}{\kappa}-\frac{A_t}{\exp\left[B_t(\kappa-\kappa_0)\right]} \tag{12}$$

$$d_c=1-\frac{\kappa_0(1-A_c)}{\kappa}-\frac{A_c}{\exp\left[B_c(\kappa-\kappa_0)\right]}. \tag{13}$$

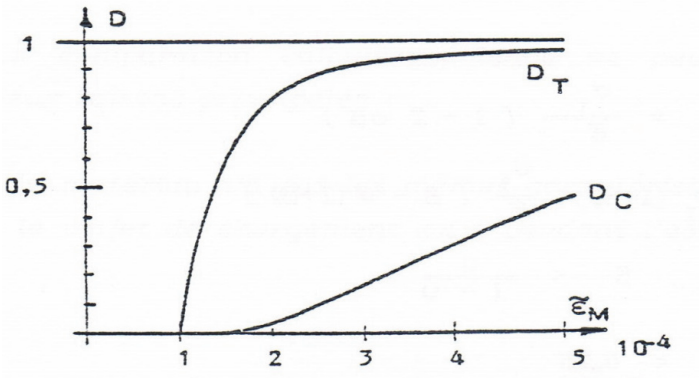

Figure 1. Evolution of two parts of damage d_t and d_c [5].

A direct tensile test or three point bend test can provide the parameters which are related to damage in tension (κ_0, A_t, B_t). Note that Eq. 7 provides a first approximation of the initial threshold of damage, and the tensile strength of the material can be deduced from the compressive strength according to standard code formulas. The parameters (A_c, B_c) are fitted from the response of the material to uniaxial compression.

DYNAMIC EQUATIONS OF MOTION

Dynamic analysis of structures exhibiting non linear behavior is performed by using direct integration, to trace the response in the time domain. The nonlinear dynamic equilibrium equation can be written as

$$M\ddot{u}_n + C\dot{u}_n + p_n = f_n \tag{14}$$

where M and C are the global mass and damping matrices respectively, p_n is the global vector of internal resisting nodal forces, f_n is the vector of consistent nodal forces for the applied body and surfaces traction forces grouped together, the body force term $(-MI\ddot{u}_g)$ due to seismic excitation, is included in the body forces which are taken into account in f_n, $\ddot{u}_n$ is the global vector of nodal accelerations and $\dot{u}_n$ is the global vector of nodal velocities [7].

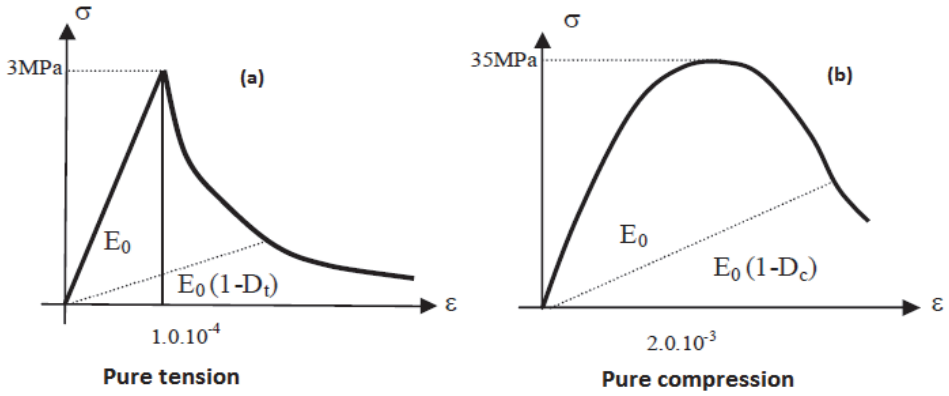

Figure 2: Uniaxial response of the model in (a) tension and (b) compression [5]

When the structure is subjected to seismic excitation, the external applied body forces is

$$f_n = -MI\ddot{u}_g \tag{15}$$

Where $\ddot{u}_g$ is ground acceleration and I is a vector indicating the direction of the earthquake excitation.

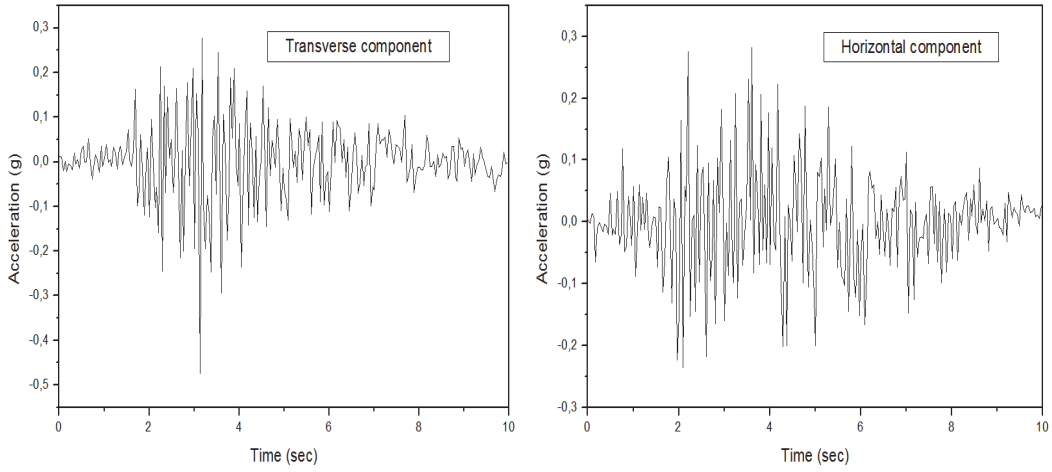

Figure 3: Koyna accelerograms a) Transverse component b) Vertical component [8].

The geometry of a typical non-overflow monolith of the Koyna dam is illustrated in Fig. 4. The monolith is 103 m high and 71 m wide at its base. The upstream wall of the monolith is assumed to be straight and vertical, which is slightly different from the real configuration. The depth of the reservoir at the time of the earthquake is h_w = 91.75 m. Following the work of other investigators, we consider a two-dimensional analysis of the non-overflow monolith assuming plane stress conditions. The finite element mesh used for the analysis is shown in Fig. 4. It consists of 760 first-order, reduced-integration, plane stress elements (CPS4R). Nodal definitions are referred to a global rectangular coordinate system centered at the lower left corner of the dam, with the vertical y-axis pointing in the upward direction and the horizontal x-axis pointing in the downstream direction. The transverse and vertical components of the ground accelerations recorded during the Koyna earthquake are shown in Fig. 3. (units of g = 9.81 m sec^{-2}). Prior to the earthquake excitation, the dam is subjected to gravity loading due to its self-weight and to the hydrostatic pressure of the reservoir on the upstream wall [8].

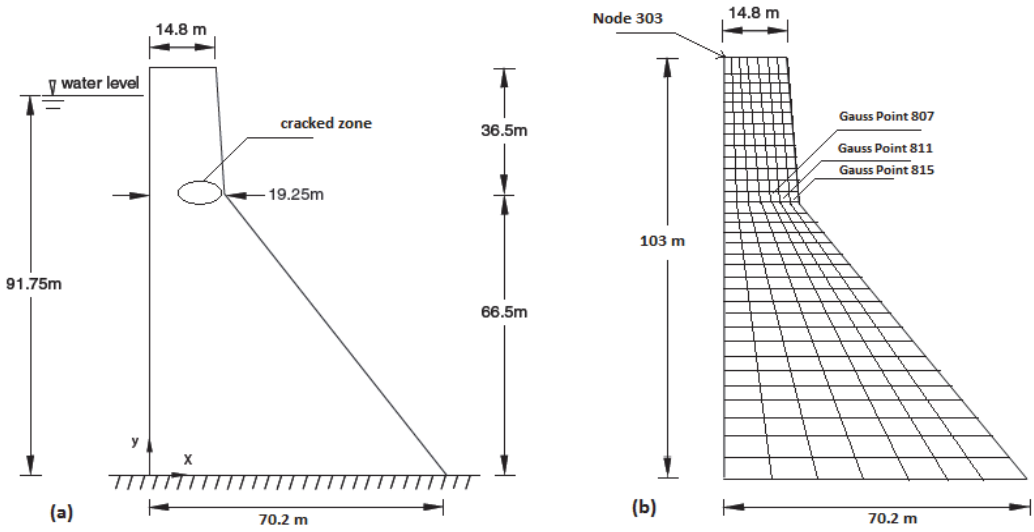

Figure 4: Geometric properties of the KOYNA dam.

Parameters used in Mazars's model for concrete	
Young modulus E	31027 MPa
Poisson's ratio ν	0.2
Mass density ρ	2643 kg/m^3
Initial damage threshold ε_{D_0}	1.5 10^{-4}
A_t	1.0
B_t	30000
A_C	1.4
B_C	1545

Table1: Material properties.

RESULTS

We note that the displacements are relatively low during the first two seconds because of low the amplitudes of the excitations. The displacements reach their maximum at 3.7 s and 7.5 s, 30 mm was recorded at 3.8 s, the maximum displacement value does not correspond to the maximum amplitude of the excitement that is recorded at 3.65 s. The nodal displacements decrease after 7.5 s.

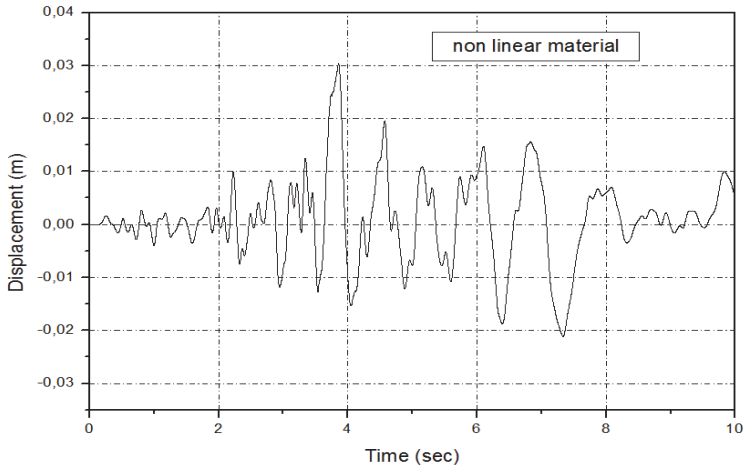

Figure 5: Horizontal displacements at the crest of the dam

We note that the displacements are relatively low during the first two seconds because of low the amplitudes of the excitations. The displacements reach their maximum at 3.7 s and 7.5 s, 30 mm was recorded at 3.8 s, the maximum displacement value does not correspond to the maximum amplitude of the excitement that is recorded at 3.65 s. The nodal displacements decrease after 7.5 s.

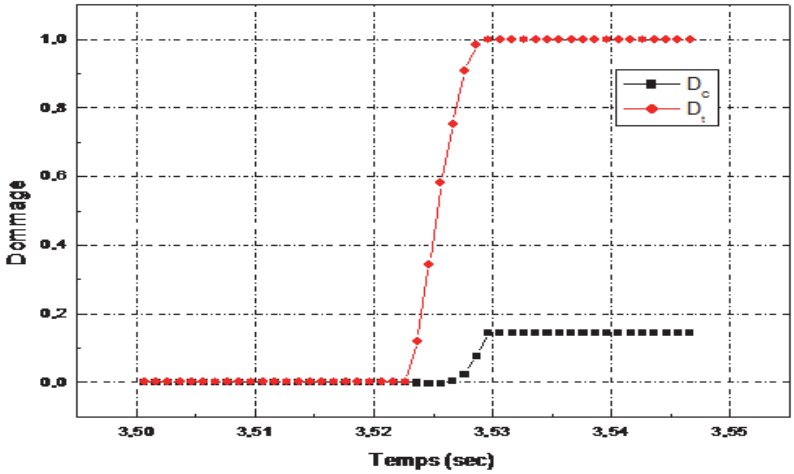

Figure 6: Damage evolution, D_t and D_c.

Fig. 6. Shows the evolution of D_t and D_c, the tensile and compressive part of the damage variable D. We note that traction damage is more significant and more predominant than in compression, which leads to a brittle fracture of the material by traction. The total rupture of the material can be achieved by traction, in compression the damage is less significant, so the rupture will not occur under compression, Fig. 1b presents some ductility of the material. It is also seen from this figure (Fig. 6) that the tensile damage starts firstly and evolves quickly to a value close to 1 ($D_t \approx 1$), then followed by the compression damage, but the temporary difference is only of the order of a thousandth of a second, so nearly or completely insignificant difference. In counterparty, compressive damage is less important, it increases until a value $D_c \approx 0.15$ a value that does not allow rupture in compression of the element.

Damage were observed (see Fig. 7) in the dam after 3.53 s at the integration point (815) of the element 204, then from 3.54 s at integration point (811) of the element 203 and finally, from 3.54 s at Gauss point (807) of the element 202. It may be noted that the evolution of the damage is mainly concentrated in the time interval where the maximum values of positive and negative displacements occur.

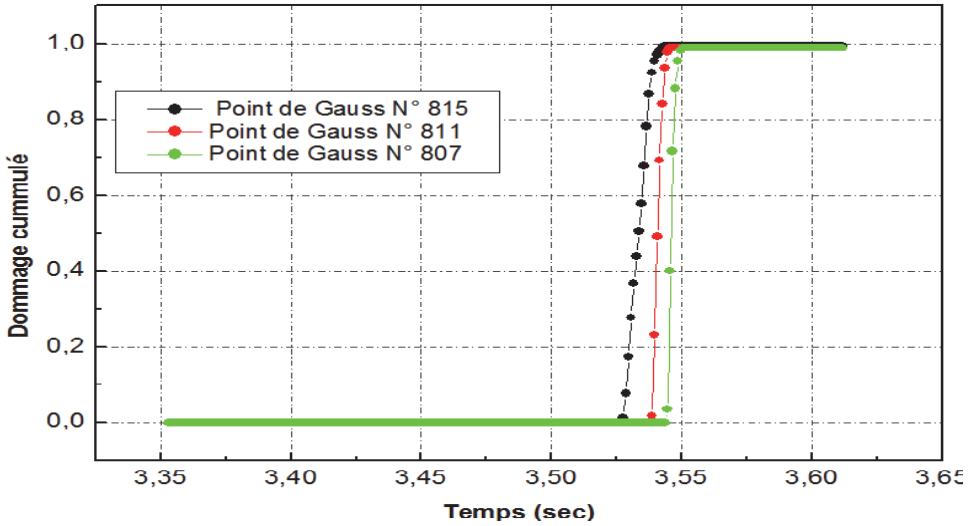

Figure 7: Damage evolution in Gauss points.

Conclusion

We have taken the example of a concrete gravity dam subjected to seismic excitation in the form of accelerograms. The results are, first the response of gravity dam subjected to seismic loading as displacements history, secondly the history of the evolution of integration points damage at the cracked or damaged zone. The dynamic equilibrium equation is solved, an integration algorithm by the method of central differences for nonlinear systems, we have used a very small time step (0.0001 s). The choice of weight Koyna dam in India is the fact that many studies have been conducted on this structure to a known destructive earthquake in 1967. The records of the earthquake accelerograms as with horizontal and vertical components were used as dynamic loads.

References

[1] Calayir, Y., Karaton, M., A continuum damage concrete model for earthquake analysis of concrete gravity dam–reservoir systems, Soil Dynamics and Earthquake engineering, 25 (2005) 857-869.
[2] Jianwen, P., Chuhann, Z., Xuyanjie, Feng, J., A comparative study of the different procedures for seismic cracking analysis of concrete dams, Soil Dynamics and Earthquake engineering, 31 (2011) 1594-1606.
[3] Calayir, Y., Karaton, M., A continuum damage concrete model for earthquake analysis of concrete gravity dam–reservoir systems. Soil Dynamics and Earthquake Engineering, 25 (2005) 857–869.
[4] Omidi, O., Valliappan, S., Lotfi, V., Seismic cracking of concrete gravity dams by plastic–damage model using different damping mechanisms. Finite Elements in Analysis and Design, 63 (2013) 80–97.
[5] Mazars, J., Application de la mécanique de l'endommagement au comportement non linéaire et à la rupture du béton de structure, Doctoral thesis, University of Paris 6, France (1984).
[6] Mazars, J., Pijaudier-Cabot, G., Continuum damage theory- application to concrete, J. Engrg. Mech. ASCE, 115 (1989) 345-365.
[7] Owen, D.R.J., Hinton, E., Finite element in plasticity, Theory and Practice. Ed. Pineridge Press Limited, (1986).
[8] ABAQUS 6.10. Example problems manual; volume I: Static and Dynamic Analyses.